Lecture Notes: The Many-Electron Problem

1 Introduction

In order to explain many important properties of materials and phenomena, it is necessary to go beyond independent-particle approximations and directly account for many-body effects resulting from electronic interactions. The many-body problem poses significant scientific challenges but has seen substantial progress due to theoretical advancements and computational improvements.

This chapter provides a brief overview of the interacting-electron problem and introduces key historical and methodological developments.

2 The Electronic Structure Problem

The behavior of atoms, molecules, and condensed matter is governed by quantum statistical mechanics, with electrons and nuclei interacting via the Coulomb potential. The essential ingredients are contained in the Hamiltonian:

$$\hat{H} = -\frac{\hbar^2}{2m_e}\sum_i \nabla_i^2 - \sum_{i,I}\frac{Z_I e^2}{|\mathbf{r}_i - \mathbf{R}_I|} + \frac{1}{2}\sum_{i\neq j}\frac{e^2}{|\mathbf{r}_i - \mathbf{r}_j|} - \sum_I \frac{\hbar^2}{2M_I}\nabla_I^2 + \frac{1}{2}\sum_{I\neq J}\frac{Z_I Z_J e^2}{|\mathbf{R}_I - \mathbf{R}_J|}. \quad (1)$$

In atomic units ($\hbar = m_e = e = 4\pi\varepsilon_0 = 1$), this simplifies to:

$$\hat{H} = \hat{T}_e + \hat{V}_{en} + \hat{V}_{ee}, \quad (2)$$

where $\hat{T}_e$ is the kinetic energy of electrons, $\hat{V}_{en}$ is the electron-nucleus interaction, and $\hat{V}_{ee}$ is the electron-electron interaction.

3 Why is the Many-Body Problem Difficult?

The primary challenge arises from the high dimensionality of the many-electron wavefunction, which depends on $3N$ variables for N electrons. A complete wavefunction cannot be factorized due to electron-electron interactions, making direct computation exponentially complex.

For instance, the number of Slater determinants required to describe the wavefunction scales as:

$$\binom{M}{N} = \frac{M!}{N!(M-N)!} \approx e^{CN}, \quad (3)$$

where M is the number of basis functions, and $C > 0$.

4 Why is the Independent-Electron Picture So Successful?

Underlying all independent-particle approaches is the idea that each electron interacts with an effective potential that mimics the effects of the other electrons. This greatly simplifies the problem, allowing the use of single-particle wavefunctions. Key reasons for the success of this approach include:

- The exclusion principle ensures electrons "see" each other, leading to Fermi-Dirac statistics.
- Symmetry and conservation laws, such as momentum conservation, play a central role in simplifying calculations.
- Independent-electron methods often provide a good starting point for describing properties such as band structures and Fermi surfaces.

Fermi liquid theory, introduced by Landau, extends the independent-electron picture to interacting systems by introducing the concept of quasi-particles, which behave like non-interacting particles near the Fermi surface. This theory assumes a one-to-one correspondence between excitations in the interacting and non-interacting systems, preserving conservation laws and providing a foundation for understanding many phenomena in condensed matter physics.

5 Development of Theoretical Approaches to the Many-Body Problem

While the independent-electron picture provides valuable insights, there are many phenomena it cannot explain, such as:

- Phase transitions, like the Wigner crystal transition, which require electron-electron interactions to explain.
- Magnetic ordering, where interactions between spins are essential.
- Screening effects, where electron correlations reduce the effective interaction strength.

The development of theoretical methods to address these issues has been driven by advances in computational techniques and analytical frameworks. Key milestones include:

- Density Functional Theory (DFT): Revolutionized materials modeling by providing an efficient way to calculate ground-state properties.
- Quantum Monte Carlo (QMC): Enabled simulations of complex systems by sampling many-body wavefunctions.
- Green's Function Methods: Allowed for the calculation of excitation spectra and response functions, providing direct links to experimentally measurable quantities.
- Diagrammatic Techniques: Methods such as the GW approximation and the Bethe-Salpeter equation were developed to treat electron correlations systematically.

Screening, a critical concept in many-body physics, is treated in methods like GW and QMC to account for electron correlations. These methods go beyond static mean-field descriptions, providing accurate predictions for a wide range of materials and phenomena.

6 Computational Scaling

The computational effort $T(N)$ required to solve the many-body problem depends on the method:

- Exact methods: $T(N) \sim e^{CN}$.
- DFT: $T(N) \sim N^2 - N^3$.
- GW approximation: $T(N) \sim N^2 - N^5$.
- QMC: $T(N) \sim N^3$.

7 What is Meant by Correlation?

Electron correlation refers to effects of electron-electron interactions beyond Hartree-Fock (HF) theory. The correlation energy is defined as:

$$E_c = E_{\text{exact}} - E_{\text{HF}}, \tag{4}$$

where E_{exact} is the exact ground-state energy, and E_{HF} is the energy obtained from HF calculations. HF theory includes the Pauli exclusion principle but assumes independent particles in a mean-field potential, neglecting dynamic and exchange-correlation effects.

Excitation energies in HF theory are approximately related to orbital energies by Koopmans' theorem, but these energies often poorly approximate experimental results due to missing correlation effects.

Static Correlation vs. Dynamic Correlation The distinction between static and dynamic correlation lies in the nature of the electronic interactions being described:

Static Correlation Static correlation arises in systems where the correct wavefunction requires a superposition of multiple degenerate or nearly degenerate electronic configurations. It is significant in:

- Systems with near-degenerate states, such as bond dissociation and transition states.
- Strongly correlated systems like Mott insulators.

Single-reference methods (e.g., Hartree-Fock) fail in such cases, and multi-reference approaches are needed. For example, as the bond in H_2 stretches, two nearly degenerate configurations arise, requiring multi-configurational methods for accurate representation.

Dynamic Correlation Dynamic correlation accounts for the rapid, instantaneous Coulomb interaction between electrons as they avoid each other in space. This type of correlation is:

- Present even in single-reference systems.
- Well-described by methods like perturbation theory or coupled-cluster techniques.

Dynamic correlation provides corrections to ground-state energies and properties in weakly correlated systems like CH_4 or benzene.

Combined Role Both static and dynamic correlation often coexist. For example:

- Static correlation dominates in strongly correlated systems and transition states.
- Dynamic correlation improves quantitative accuracy for weakly correlated systems.

7.1 Strongly Correlated Systems: High-T_c Superconductors

Strongly correlated systems, such as high-T_c superconductors, are primarily governed by **static correlation**, although **dynamic correlation** also plays an important role.

Static Correlation

- Static correlation dominates because electrons in these systems are strongly localized due to the Coulomb repulsion in partially filled d- or f-orbitals.
- This type of correlation explains phenomena such as Mott insulating behavior in the undoped parent compounds and antiferromagnetic ordering.
- Models like the Hubbard and t-J models capture the competition between localization (due to strong U) and delocalization (hopping t).
- The pseudogap phase observed in underdoped cuprates arises largely from static correlation effects.

Dynamic Correlation

- Dynamic correlation becomes significant when doping introduces itinerant carriers into the system, as these electrons dynamically interact with each other and with localized states.
- It plays a key role in the renormalization of quasiparticle properties, such as effective mass and spectral weight near the Fermi level.

Combined Picture While static correlation underpins the magnetic and insulating properties of undoped parent compounds, dynamic correlation contributes to the emergence of superconductivity upon doping. Both types of correlation are essential for understanding the unconventional pairing mechanisms and anomalous properties of high-T_c superconductors.

7.2 Symmetry and Restricted Solutions

Unrestricted Hartree-Fock (UHF) allows symmetry breaking in the wavefunction to lower the energy, capturing part of the correlation. However, the correlation energy is conventionally measured relative to restricted Hartree-Fock (RHF) to ensure consistency, as RHF enforces the symmetries of the Hamiltonian.

7.2.1 Difference Between Restricted and Unrestricted Hartree-Fock

The Restricted Hartree-Fock (RHF) and Unrestricted Hartree-Fock (UHF) methods are two variations of the Hartree-Fock approximation, differing in how they treat the spin of electrons in a system.

Restricted Hartree-Fock (RHF):

- Assumes that each spatial orbital is doubly occupied, meaning both spin-up and spin-down electrons share the same spatial orbital.
- This is appropriate for systems where the electrons are paired, such as closed-shell systems with no unpaired electrons.
- The RHF wavefunction is a single Slater determinant, and the total spin of the system is strictly zero.
- **Limitation:** RHF fails to accurately describe systems with strong spin polarization, such as open-shell molecules, radicals, or magnetic systems, where unpaired electrons require distinct spatial orbitals.

Unrestricted Hartree-Fock (UHF):

- Allows spatial orbitals for spin-up and spin-down electrons to differ, enabling a more flexible description of the electronic structure.
- This is crucial for systems with unpaired electrons, such as radicals, open-shell molecules, and magnetic systems.
- The UHF wavefunction is no longer a pure spin eigenstate but can describe spin-polarized systems more accurately.
- **Limitation:** The lack of spin purity introduces "spin contamination," where the wavefunction contains contributions from states with higher spin multiplicities.

Comparison:

- RHF is simpler and computationally cheaper, but it is limited to systems where electrons are paired and spin-unpolarized.
- UHF provides a more accurate description for spin-polarized systems but may require post-Hartree-Fock corrections to address spin contamination.

8 Signatures of Correlation

8.1 Band Structures and the Bandgap Problem

The concept of a band structure is a central result of independent-particle theories, representing the energy levels of electrons in a periodic lattice. However, the "bandgap problem" arises because experimental bandgaps are often poorly reproduced by these methods. For instance, Kohn-Sham eigenvalues in Density Functional Theory (DFT) systematically underestimate the bandgap, sometimes predicting semiconductors like Ge to be metallic.

Hartree-Fock, on the other hand, overestimates the bandgap due to the neglect of screening effects. A more accurate description involves methods like the GW approximation, where dynamic screening of the electron-electron interaction is included. Experimental results for Ge, comparing DFT, GW, and Hartree-Fock band structures, show the importance of including correlation effects to accurately reproduce measured gaps and bandwidths (refer to Fig fig:2.6).

In addition to bandgaps, correlation affects the lifetime of electronic states. Broadened spectral peaks observed in photoemission and inverse photoemission experiments indicate finite lifetimes, which cannot be captured by independent-particle theories.

8.2 Ground-State and Thermodynamic Properties

Ground-state properties, such as binding energies and equilibrium geometries, are sensitive to electron correlation. For example, in the hydrogen molecule, correlation contributes about 1 eV to the total binding energy of ≈ 5 eV. Similarly, the atomic volumes of lanthanides and actinides reflect the contrast between localized $4f$ and delocalized $5d$ electrons, as illustrated in Fig fig:2.1.

Thermodynamic properties, such as the bulk modulus and dielectric constants, also depend critically on correlation. These properties are often underestimated in mean-field calculations without proper treatment of electron-electron interactions.

8.3 Van der Waals Forces

Van der Waals interactions arise purely from correlation effects. These forces, which decay as R^{-6} with interatomic distance R, stabilize weakly bonded systems such as rare gas solids and biological structures. For example, simulations of biopolymers show that van der Waals forces are critical for maintaining compact structures like the α-helix at high temperatures.

8.4 Magnetism

Magnetism is intrinsically tied to electron correlation. In ferromagnetic metals like Fe and Ni, local magnetic moments persist even above the Curie temperature T_c, where the material is no longer magnetically ordered. The magnetic susceptibility follows the Curie-Weiss law:

$$\chi(T) = \frac{\mu_{\text{eff}}^2}{3(T - T_c)}, \tag{5}$$

where μ_{eff} is the effective magnetic moment. The coexistence of band-like and localized behaviors highlights the role of correlation in itinerant magnetism.

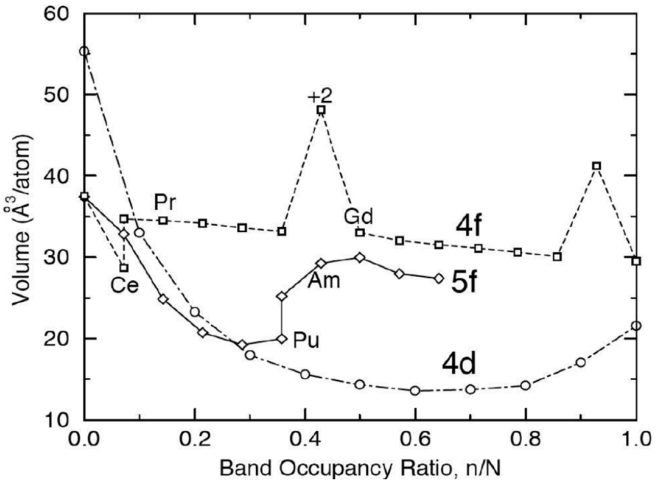

Figure 2.1. Volume per atom of the lanthanides ($4f$) and actinides ($5f$) compared with $4d$ transition metals as a function of fractional occupation of the d or f states. The smooth parabolic curve for the $4d$ series indicates a gradual filling of the d bands with maximum bonding at half-filling. In contrast, the $4f$ series lanthanides retain atomic-like character with little effect on the volume as the f shell is filled. (The jumps for Eu and Yb also support the atomic-like picture with non-monotonic changes in $4f$ occupation, denoted by the label "+2," due to added stability of the half-filled and the filled shells.) The anomalous elements are Ce and Pu; both have complex phase diagrams (see Fig. 20.1 for Ce), spectra (e.g., Fig. 2.9), and magnetic properties that are prototypes of strong interactions and signatures of correlation. (Figure provided by A. K. McMahan.)

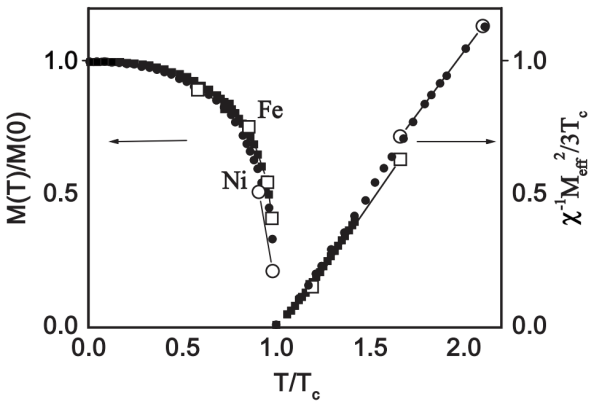

Figure 2.3. Magnetization (left curve) and magnetic susceptibility (right curve) of the $3d$ transition metals Fe (squares) and Ni (circles). Closed symbols are experiment and open symbols are from calculations [55], as discussed in Ch. 19. The curves have been normalized to the zero-temperature magnetization $M(0)$ and transition temperature T_c = 1043 K and 631 K for Fe and Ni, respectively. At low temperature, these are metals with delocalized states near the Fermi energy. Above the Curie temperature, however, the magnetic susceptibility indicates that these materials act as a collection of thermally disordered atomic-like moments. The fact that these two types of behavior occur in the same material is a signature of correlation among the electrons. To capture such effects is a goal of dynamical mean-field theory, Chs. 16–21. (From [55].)

8.5 Electron Addition and Removal: The Bandgap Problem and Beyond

Electron addition and removal processes provide direct insights into electronic structure and correlation effects. These processes are observed experimentally through photoemis-

sion spectroscopy (PES) and inverse photoemission spectroscopy (IPES). In theory, the bandgap in materials is determined by the energy difference between adding and removing an electron:

$$E_{\text{gap}} = [E(N+1) - E(N)] - [E(N) - E(N-1)]\,, \tag{6}$$

where $E(N)$ represents the ground-state energy of a system with N electrons.

The Bandgap Problem Independent-particle approximations often fail to accurately predict bandgaps:

- **Kohn-Sham DFT:** Bandgaps are systematically underestimated, sometimes predicting materials like Ge to be metallic.
- **Hartree-Fock (HF):** Overestimates bandgaps due to neglect of screening, leading to unphysically large gaps.
- **GW Approximation:** Includes dynamic screening of electron interactions and provides more accurate bandgaps, closely matching experimental results. For example, GW calculations successfully reproduce the measured band structure of Ge (refer to Fig fig:2.6).

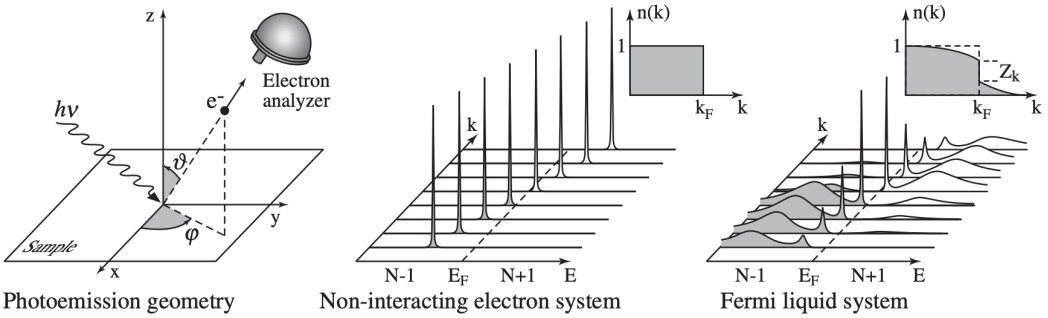

Figure 2.5. Schematic illustration of ARPES. The middle figure shows an independent-particle spectrum of δ-functions with occupation 1 or 0. The right figure exemplifies a spectrum for interacting electrons with "quasi-particle" peaks (i.e., peaks due to dressed one-particle excitations) having fractional weight and "satellites" or "sidebands" due to additional excitations that are induced in the system. Examples for satellites in photoemission are shown in Figs. 2.8 and 2.9 for plasmons in Na and atomic-like excitations in Ce, and throughout the following chapters. The insets depicting occupation numbers $n(k)$ are discussed in more detail in Secs. 5.2 and 7.5. (Provided by A. Damascelli, similar to figure in [59].)

Lifetimes and Satellites Correlation effects also manifest in broadened spectral peaks and satellite features in PES and IPES:

- Broadened peaks indicate finite lifetimes of quasiparticles due to interactions.
- Satellites, such as plasmon peaks in sodium, arise from collective excitations triggered by the photoemission process (refer to Fig fig:2.8).

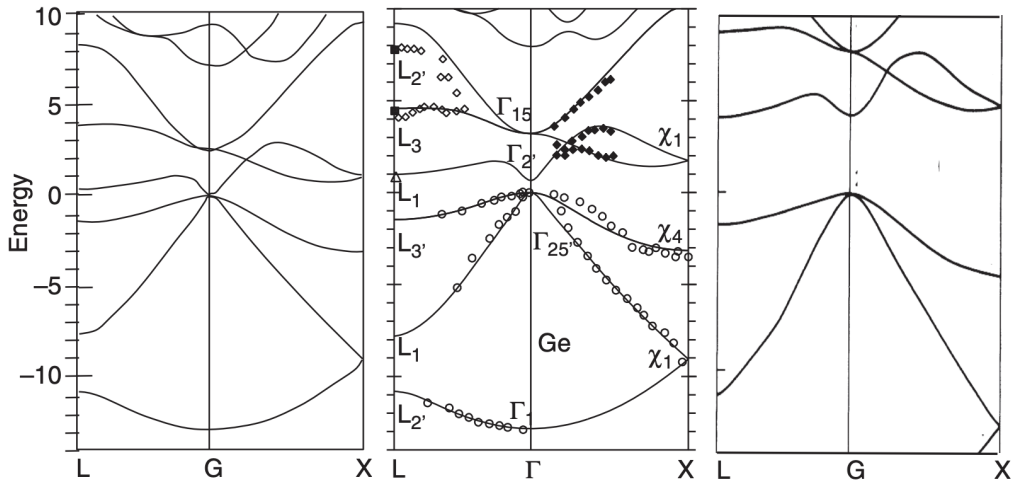

Figure 2.6. Bands of Ge from photoemission [60] and inverse photoemission [61] measurements (circle symbols in the middle panel) and from calculations in the local density (left), GW [62] (middle), and Hartree–Fock [63] (right) approximations. The LDA results, based on the assumption that the Kohn–Sham eigenvalues can be interpreted as addition and removal energies, are dramatically wrong: they give Ge as a metal. In contrast, the Hartree–Fock bands [63] have gaps that are much too large. This sets the theoretical challenge to go beyond Hartree–Fock and include screening; more recent GWA calculations (Ch. 13) provide remarkably accurate results for a large range of materials, as shown in Fig. 13.5.

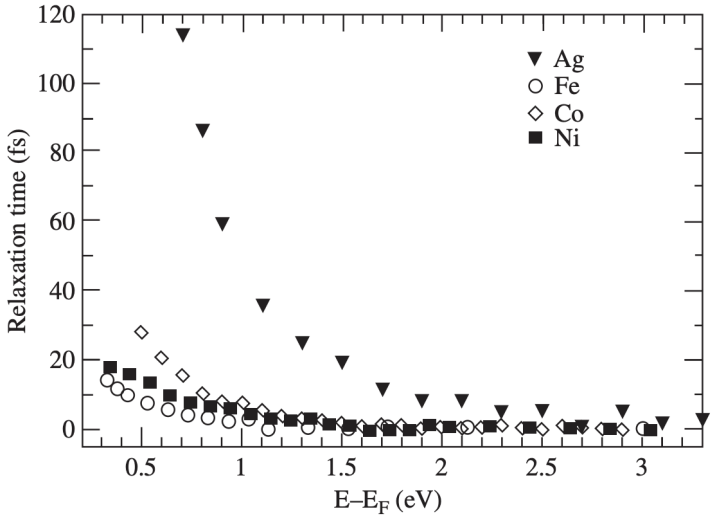

Figure 2.7. Electron lifetimes in transition metals measured with two-photon photoemission. The fact that the lifetime away from the Fermi level is finite can only be explained with interactions. Note that the lifetimes are much shorter in the transition metals that have narrow *d* bands at the Fermi level and display many other phenomena linked to correlation. (From [64].)

Band Structures Experimental techniques like angle-resolved photoemission spectroscopy (ARPES) provide detailed information about band structures. The agreement

between GW-calculated band structures and ARPES measurements highlights the importance of incorporating electron correlation.

Beyond the Independent-Particle Picture Spectra often reveal features that cannot be explained within the independent-particle framework. For instance:

- Excitonic effects shift optical absorption peaks below the fundamental bandgap (see Fig fig:2.10).
- Strong interactions in correlated systems can split bands, as observed in Mott insulators and heavy fermion systems.

These observations underscore the limitations of mean-field theories and the necessity of many-body approaches to accurately describe electronic excitations.

8.6 Excitons and Optical Spectra

Electron-hole interactions due to correlation give rise to excitons, or bound electron-hole pairs. These states are responsible for optical absorption peaks below the bandgap energy, as seen in materials like lithium fluoride (LiF). Excitons can be modeled using the Bethe-Salpeter equation, which includes the effects of electron-hole interactions beyond independent-particle approximations (refer to Fig fig:2.10 for LiF optical spectra).

8.7 Satellites and Sidebands

In addition to broadening and finite lifetimes in spectral peaks, many materials exhibit distinct satellite or sideband features in their photoemission and inverse photoemission spectra. These features are a direct consequence of electron-electron interactions and cannot be explained within an independent-particle framework.

Plasmons Plasmons, which are collective oscillations of the electron gas, often manifest as additional peaks or satellites in the spectra. For example, in sodium, the photoemission spectrum shows distinct peaks at energy intervals corresponding to one and two plasmon energies beyond the main quasiparticle peak. These plasmon satellites arise from the interaction of the photoemission hole with the surrounding electron gas (refer to Fig fig:2.8). Their presence is a qualitative signature of strong correlation effects, even in simple metals like sodium.

Atomic-Like Interactions Materials with partially filled f states, such as the lanthanides and actinides, exhibit even more pronounced satellite features. For example, the photoemission spectra of cerium show two peaks, one below the Fermi energy and one at higher energy, corresponding to Hubbard bands. These peaks are separated by the on-site Coulomb interaction U, indicating strong atomic-like interactions among f electrons. Multiplet structures also contribute to the splitting, reflecting the complex interplay of spin and orbital degrees of freedom.

Interference Effects Care must be taken in interpreting satellite intensities, as they can include contributions from extrinsic effects, such as plasmon excitation during the photoelectron's escape from the material. These extrinsic effects interfere with intrinsic satellite features, complicating the analysis.

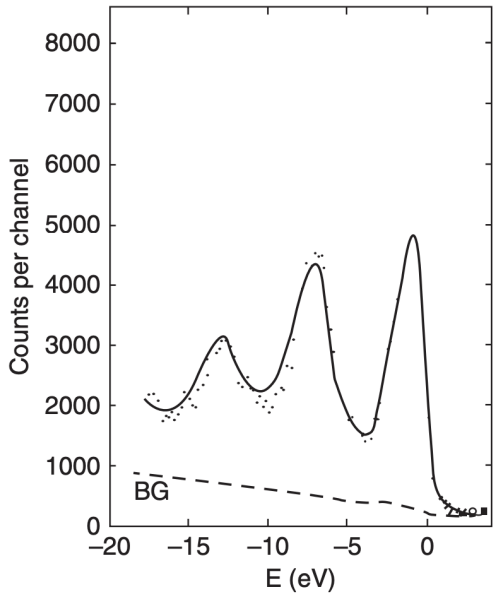

Figure 2.8. Experimental photoemission spectrum of bulk sodium (from [67]). The spectrum exhibits a quasi-particle band close to the Fermi level, and two prominent satellites between -5 and -15 eV that stem from plasmon excitations and cannot be explained in any independent-particle picture.

Applications to Materials The study of satellites provides insight into material properties. For instance, plasmon satellites help determine the effective screening in metals, while Hubbard bands and multiplet features reveal the strength of electron-electron interactions in strongly correlated systems. The distinction between quasiparticles and satellites is critical for understanding the electronic structure of transition metal oxides, heavy fermion compounds, and other correlated materials.

8.8 Particle–Hole and Collective Excitations

Spectroscopic experiments often involve exciting a system without adding or removing electrons. For example, optical absorption promotes an electron into an empty conduction state, leaving behind a hole. This process is governed by the joint density of states of valence and conduction bands in the independent-particle picture.

Excitonic Effects Observations deviate significantly from the independent-particle model due to electron-hole interactions. These interactions can lower excitation energies and create bound states known as excitons. For instance, in lithium fluoride (LiF), strong excitonic peaks appear within the bandgap, as shown in Fig. fig:2.10. These excitonic effects are well-described using the Bethe-Salpeter equation, which incorporates electron-hole correlation.

Inelastic Scattering Techniques such as inelastic X-ray scattering (IXS) and electron energy loss spectroscopy (EELS) reveal details about particle-hole excitations. These experiments measure the dynamical structure factor $S(q, \omega)$, capturing features like plasmon peaks and excitonic resonances. For example, in nickel oxide (NiO), dipole-forbidden

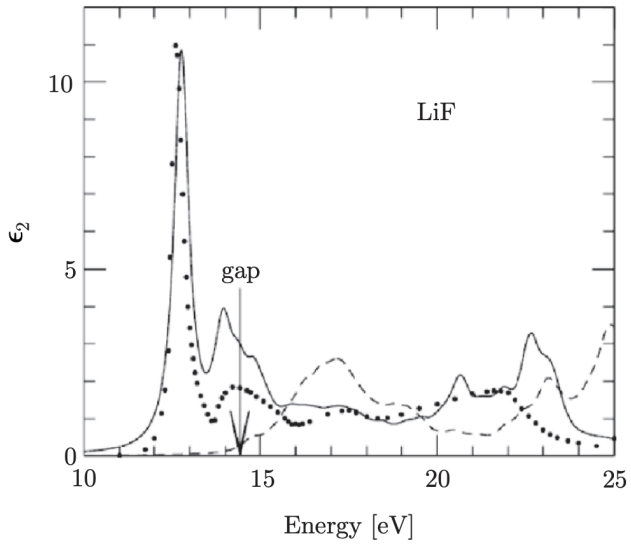

Figure 2.10. Optical spectrum of the wide-bandgap insulator LiF. The dots are experimental data from [70], the arrow indicates the quasi-particle bandgap that can be obtained from electron addition and removal spectroscopy, Eq. (2.1). The peaks at energies below the quasi-particle gap cannot be explained by a model with non-interacting quasi-particles. Calculations including the electron–hole interaction via the solution of the Bethe–Salpeter equation [71] (continuous line, see Ch. 14) reproduce the experimental peak inside the gap. Neglecting (dashed line) this interaction, the peak is absent.

excitations appear as double peaks within the bandgap.

Collective Excitations Long-range Coulomb interactions lead to collective oscillations in the electron gas, such as plasmons. These collective modes dominate the loss spectrum and differ significantly from single-particle excitations. For example, silicon exhibits distinct differences between absorption and loss spectra, highlighting the importance of collective effects.

9 Advanced Correlation Phenomena

9.1 The Kondo Effect and Heavy Fermions

The Kondo effect is a classic example of a low-energy phenomenon driven by strong correlation. It arises in metals with magnetic impurities, where conduction electrons scatter off localized impurity spins. This interaction becomes more pronounced at low temperatures, leading to a resistance minimum.

Kondo Temperature The Kondo temperature T_K characterizes the onset of this correlated state. Experimentally, scanning tunneling microscopy (STM) reveals a resonance peak near the Fermi energy, corresponding to the Kondo effect. The temperature dependence of T_K varies dramatically across materials, as shown in Fig fig:2.13.

Table 2.2. Specific heat coefficient $\gamma = C_v/T$ of some heavy fermion materials compared with Na and Pd [87]

Crystal	Na	Pd	$CeCu_2Si_2$	UBe_{13}	$CeAl_3$
γ (mJ mole^{-1} K^{-2})	1.5	10	1000	1100	1620

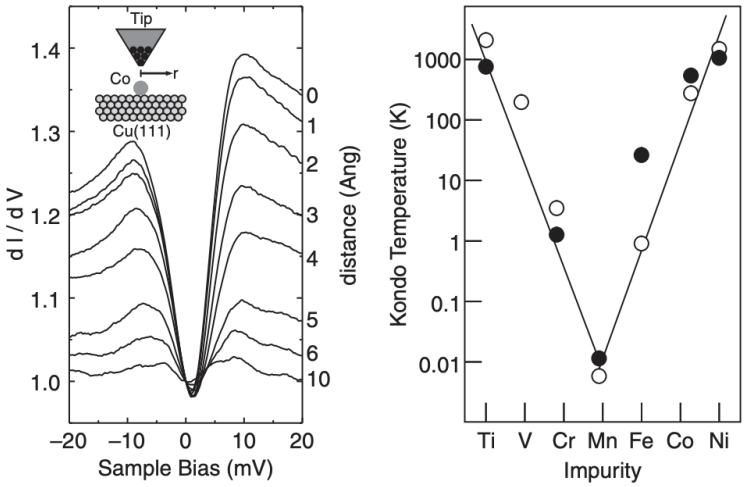

Figure 2.13. Left: spectrum of dI/dV vs. voltage V measured by STM at 4 K near a single Co atom on a Cu(111) surface. The form is that expected for the Kondo resonance and the effect is maximum if the tip is directly over the Co atom (top curve) and decreases with distance from the Co atom shown on the right vertical axis (in Angstrom). Fits to a theoretical form for a large sampling of Co atoms yields a Kondo temperature of $T_K \approx 53$ K. (From [80].) Right: Kondo temperatures for the series of $3d$ transition metals in Cu (filled circles) and Au (open circles) hosts. Note the extremely large variation interpreted as the exponential dependence of the Kondo temperature on the material parameters (see text). (From [81].)

Heavy Fermion Systems In strongly correlated materials like cerium compounds, the Kondo effect plays a central role. For example, $CeAl_3$ exhibits a large specific heat coefficient γ, reflecting the narrow bandwidth of f-electrons and their hybridization with conduction electrons. These heavy fermion systems bridge the behavior of localized moments and itinerant quasiparticles.

9.2 Mott Insulators and Metal–Insulator Transitions

Mott insulators are systems where strong correlations prevent conduction, even when bands are partially filled. This behavior is distinct from band insulators and is driven by electron-electron interactions.

Mott Transitions Transitions from insulating to metallic states can occur due to temperature, pressure, or doping. In V_2O_3, increasing pressure induces a transition from an antiferromagnetic insulator to a paramagnetic metal, as shown in Fig fig:2.14 The transition is first-order, with a critical endpoint analogous to liquid-gas phase transitions.

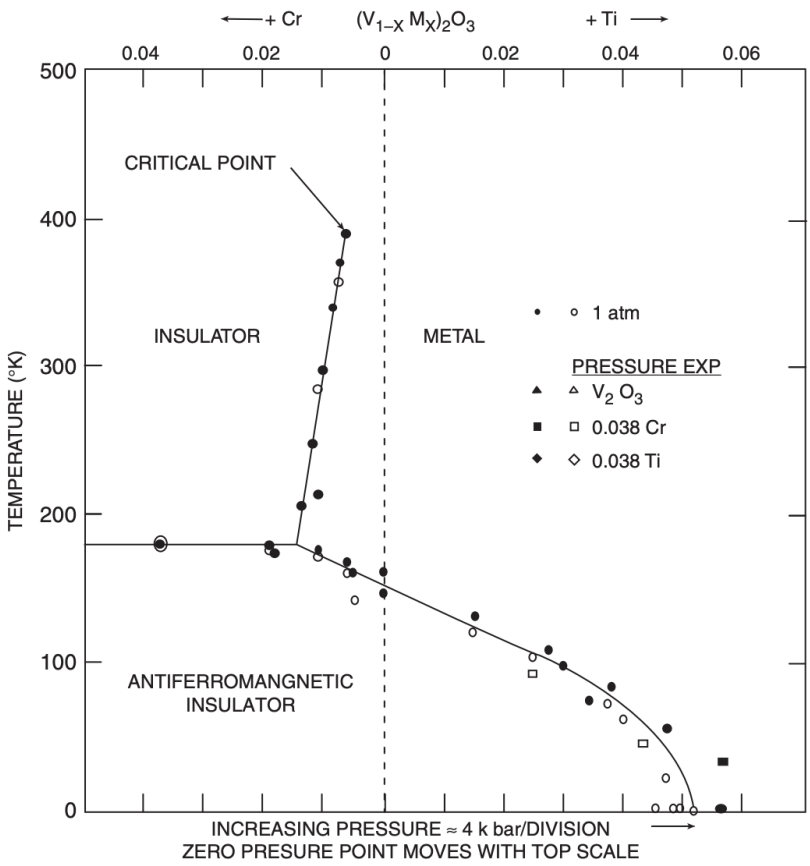

Figure 2.14. Phase diagram of $(V_{1-x}\,M_x)_2O_3$ as a function of pressure or doping with M denoting Cr or Ti. With the addition of $\approx 1\%$ Cr (argued to act like a negative pressure) there is a first-order transition that ends in a critical point. This has the characteristics expected for a Mott transition; however, there are many possible mechanisms as described in the text and Sec. 20.6. (From [90].)

Doping Effects Doping a Mott insulator introduces carriers that disrupt the insulating state. For example, in nickel oxide (NiO) doped with lithium, spectral weight shifts from the conduction band to the valence band, effectively collapsing the gap.

Applications to High-Temperature Superconductors Mott physics underpins phenomena in high-temperature superconductors. In cuprates, doping transforms the parent antiferromagnetic insulator into a superconductor. ARPES experiments reveal pseudogaps and other anomalous features, emphasizing the interplay between doping and correlation.

9.3 Reduced Dimensionality

Lower-dimensional systems, such as chains or planes, amplify correlation effects due to enhanced localization and reduced screening. High-temperature superconductors like cuprates exhibit phenomena such as the pseudogap, where parts of the Fermi surface disappear. ARPES measurements reveal the momentum-resolved electronic structure, providing insights into the interplay between dimensionality and correlation.

9.4 Lower Dimensions: Stronger Interaction Effects

Strongly correlated behavior becomes more pronounced in systems with reduced dimensionality. In low-dimensional systems, the interplay between enhanced localization and reduced screening intensifies correlation effects. Examples include:

- **High-temperature superconductors:** Cuprates with planar CuO_2 layers display complex behaviors, such as pseudogaps near the Fermi surface.
- **Quasi-1D systems:** Systems like organic conductors exhibit pronounced fluctuations due to strong correlations.

Angle-resolved photoemission spectroscopy (ARPES) experiments provide momentum-resolved views of such systems, highlighting the deviations from Fermi-liquid theory.

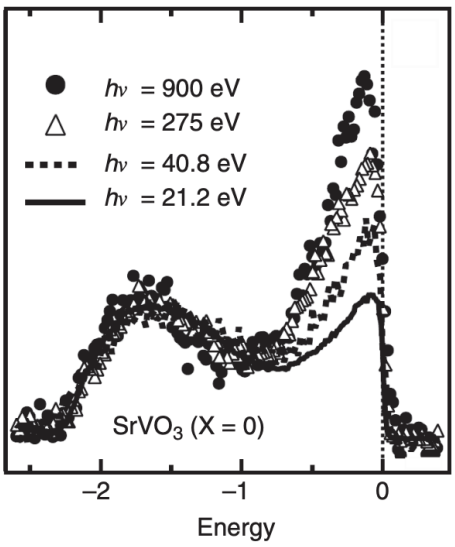

Figure 2.17. Photoemission spectra for the $3d$ states in $SrVO_3$ as a function of the photon energy [100]. The spectra are normalized by the incoherent spectral weight. With increasing photon energy the experiment becomes more bulk sensitive and the quasi-particle/satellite ratio increases, suggesting weaker correlation effects. Similar studies were done for other vanadates [100] and for V_2O_3 [93, 101] to establish that the data in Fig. 2.15 are for the bulk. (From [100].)

and 2.8. The quantity of interest is the ratio between the quasi-particle and sideband intensities, as a measure of the importance of interactions. A strong photon energy dependence can be observed. The data for the highest photon energy is most representative of the bulk. Since the sideband-over-quasi-particle ratio is highest at the lowest photon energy (most surface sensitive), this suggests that, as intuitively expected, interaction effects are stronger at the surface than in the bulk.

10 Concepts and Models for Interacting Electrons

This chapter introduces idealized models and theoretical concepts that form the foundation of interacting-electron studies. These include the Wigner and Mott transitions,

the Hubbard model, Fermi liquid theory, and localized spin models. These models help explain phenomena such as quasi-particles, collective excitations, and the behavior of electrons in strongly correlated systems.

10.1 The Wigner Transition and the Homogeneous Electron System

The homogeneous electron gas (HEG) is the simplest model of interacting electrons, consisting of electrons in a uniform positive charge background. The Hamiltonian for the HEG in atomic units is:

$$\hat{H} = -\frac{1}{2}\sum_i \nabla_i^2 + \frac{1}{2}\sum_{i\neq j}\frac{1}{|\mathbf{r}_i - \mathbf{r}_j|} + E_0, \tag{7}$$

where E_0 accounts for the neutralizing background.

The electron density is characterized by the parameter r_s, defined by $4\pi r_s^3/3 = 1/n$, where n is the electron density. The HEG is used extensively in density functional theory and quantum Monte Carlo calculations.

Wigner Crystal Formation At low densities (large r_s), the potential energy dominates, and the system forms a Wigner crystal to minimize potential energy. At high densities (small r_s), the kinetic energy dominates, and the system behaves as a non-interacting Fermi gas. The phase diagram of the HEG, as shown in Fig. 3.1, highlights these regimes.

Phase Transitions The transition between the Wigner crystal and Fermi gas phases is a pure example of a Mott transition, driven solely by electron-electron interactions. Additional phases, such as polarized fluids and superconducting phases, can occur at intermediate densities.

10.2 The Mott Transition and the Hubbard Model

The Mott transition describes the metal-insulator transition driven by electron interactions. Mott argued that in a crystalline array of hydrogen atoms, a critical lattice constant determines whether the system behaves as a metal or insulator. This transition depends on the ratio U/W, where U is the interaction energy, and W is the bandwidth.

The Hubbard Model The Hubbard model is a simplified representation of interacting electrons on a lattice. Its Hamiltonian is:

$$\hat{H} = \sum_{i,\sigma}\epsilon_0\hat{n}_{i\sigma} + \frac{U}{2}\sum_i \hat{n}_{i\uparrow}\hat{n}_{i\downarrow} - \sum_{i\neq j,\sigma} t_{ij}\hat{c}^\dagger_{i\sigma}\hat{c}_{j\sigma}, \tag{8}$$

where t_{ij} represents the hopping parameter, U is the on-site interaction, and $\hat{n}_{i\sigma}$ is the number operator.

The Hubbard model exhibits a Mott transition at half-filling, with insulating behavior at large U/t. Solutions for 1D systems using the Bethe ansatz provide benchmarks for approximations such as DMFT.

10.3 The Two-Site Hubbard Model (Hubbard Dimer)

The two-site Hubbard model, also known as the Hubbard dimer, is the simplest non-trivial case of the Hubbard model. It captures essential features of interacting electrons and serves as a benchmark for approximations.

10.3.1 Hamiltonian

The Hamiltonian for the two-site Hubbard model is:

$$\hat{H} = -t \sum_{\sigma} \left(\hat{c}_{1\sigma}^{\dagger} \hat{c}_{2\sigma} + \hat{c}_{2\sigma}^{\dagger} \hat{c}_{1\sigma} \right) + U \left(\hat{n}_{1\uparrow} \hat{n}_{1\downarrow} + \hat{n}_{2\uparrow} \hat{n}_{2\downarrow} \right), \tag{9}$$

where t is the hopping parameter, U is the on-site interaction energy, and $\hat{c}_{i\sigma}^{\dagger}$ ($\hat{c}_{i\sigma}$) are the electron creation (annihilation) operators at site i with spin σ.

10.3.2 Solutions for Different Electron Numbers

Zero and One Electron Cases: For zero electrons, the system has no interactions or hopping, so $E = 0$. For one electron, the solutions are simple bonding and antibonding states with energies:

$$E = \pm t. \tag{10}$$

Two-Electron Case: The two-electron case is more complex and involves singlet and triplet states:

- **Triplet States:** The triplet states are:

$$\psi_{\text{triplet}} = \frac{1}{\sqrt{2}} \left(\hat{c}_{1\uparrow}^{\dagger} \hat{c}_{2\uparrow}^{\dagger} + \hat{c}_{1\downarrow}^{\dagger} \hat{c}_{2\downarrow}^{\dagger} \right) |0\rangle, \tag{11}$$

  with energy $E = 0$ since there is no double occupancy.

- **Singlet States:** The singlet states involve configurations with double occupancy. The energies are:

$$E = \frac{U}{2} \pm \sqrt{4t^2 + \left(\frac{U}{2} \right)^2}. \tag{12}$$

  The ground state is a singlet with energy decreasing as U increases.

10.3.3 Insights

The Hubbard dimer illustrates the interplay between hopping and on-site interaction. In the large-U limit, the system behaves like a Heisenberg spin model with antiferromagnetic coupling:

$$J = \frac{4t^2}{U}. \tag{13}$$

At small U, the bonding-antibonding picture dominates, while at large U, the interaction localizes electrons.

10.4 Magnetism and Spin Models

Spin models describe localized magnetic moments, with the Heisenberg model being a common representation:

$$\hat{H} = -\sum_{i<j} J_{ij} \hat{\mathbf{S}}_i \cdot \hat{\mathbf{S}}_j, \tag{14}$$

where J_{ij} represents exchange constants. At large U, the Hubbard model reduces to a spin model with $J \propto t^2/U$.

Monte Carlo methods show antiferromagnetic order in the ground state for 2D systems at $T = 0$, with reduced moments due to quantum fluctuations.

10.5 Normal Metals and Fermi Liquid Theory

Fermi liquid theory (FLT) explains the behavior of interacting electrons in metals as quasi-particles with renormalized properties. The energy of the system can be expanded as:

$$E - E_0 = \sum_{k,\sigma} \frac{\delta E}{\delta n_{k,\sigma}} \delta n_{k,\sigma} + \frac{1}{2} \sum_{k,\sigma,k',\sigma'} f^{\sigma\sigma'}(k,k') \delta n_{k,\sigma} \delta n_{k',\sigma'} + \ldots, \tag{15}$$

where $f^{\sigma\sigma'}(k,k')$ represents the quasi-particle interaction.

Key properties, such as the specific heat and magnetic susceptibility, are determined by renormalized parameters like the effective mass m^*. FLT also extends to charged systems, incorporating screening effects.

10.6 The Kondo Problem

The Kondo problem describes the interaction between conduction electrons and a localized magnetic impurity in a metal. This interaction leads to unconventional low-temperature behavior, such as an increase in resistance below a characteristic temperature T_K, known as the Kondo temperature.

10.6.1 Hamiltonian for the Kondo Model

The simplest model for the Kondo problem is:

$$\hat{H}_{\text{Kondo}} = \sum_{\mathbf{k},\sigma} \epsilon_{\mathbf{k}} \hat{c}^\dagger_{\mathbf{k}\sigma} \hat{c}_{\mathbf{k}\sigma} + J \sum_{\mathbf{k},\mathbf{k}'} \hat{S} \cdot \hat{s}_{\mathbf{k}\mathbf{k}'}, \tag{16}$$

where:

- $\hat{c}^\dagger_{\mathbf{k}\sigma}$ ($\hat{c}_{\mathbf{k}\sigma}$) are creation (annihilation) operators for conduction electrons with momentum $\mathbf{k}$ and spin σ.
- J is the exchange coupling between the localized impurity spin $\hat{S}$ and the conduction electron spin density $\hat{s}_{\mathbf{k}\mathbf{k}'}$.
- $\hat{s}_{\mathbf{k}\mathbf{k}'} = \frac{1}{2} \sum_{\alpha\beta} \hat{c}^\dagger_{\mathbf{k}\alpha} \boldsymbol{\sigma}_{\alpha\beta} \hat{c}_{\mathbf{k}'\beta}$ is the spin density operator for the conduction electrons, where $\boldsymbol{\sigma}$ are the Pauli matrices.

10.6.2 Physical Phenomena

At high temperatures, the impurity behaves as a free magnetic moment, contributing to a Curie-like magnetic susceptibility:

$$\chi(T) = \frac{C}{T}, \tag{17}$$

where C is the Curie constant. However, as the temperature decreases below T_K, the impurity spin becomes screened by the conduction electrons, forming a many-body singlet state. This phenomenon is known as the Kondo effect.

10.6.3 Kondo Temperature

The Kondo temperature T_K is the energy scale below which the Kondo effect dominates. It is given by:

$$T_K \propto D \exp\left(-\frac{1}{J\rho}\right), \tag{18}$$

where:

- D is the conduction electron bandwidth (high-energy cutoff).
- ρ is the density of states at the Fermi level.

10.6.4 Low-Temperature Properties

At $T \ll T_K$, the system exhibits:

- A saturated resistivity due to unitary scattering off the impurity.
- A specific heat contribution $C \propto T$ associated with the formation of the singlet state.
- A Pauli-like magnetic susceptibility, indicating the absence of a free moment.

10.6.5 Anderson Impurity Model and Connection to the Kondo Problem

The Kondo problem can also be derived as a low-energy limit of the Anderson impurity model, which describes a localized state hybridizing with conduction electrons. The Anderson Hamiltonian is:

$$\hat{H}_{\text{AIM}} = \sum_{k,\sigma} \epsilon_k \hat{c}^\dagger_{k\sigma} \hat{c}_{k\sigma} + \epsilon_d \sum_\sigma \hat{n}_{d\sigma} + U \hat{n}_{d\uparrow} \hat{n}_{d\downarrow} + \sum_{k,\sigma} \left(V_k \hat{c}^\dagger_{k\sigma} \hat{d}_\sigma + \text{h.c.} \right), \tag{19}$$

where:

- ϵ_d is the energy of the localized impurity state.
- U is the on-site Coulomb repulsion.
- V_k is the hybridization between the impurity and conduction electrons.

At low energies, the Anderson impurity model maps onto the Kondo model, with an effective exchange coupling J given by:

$$J \propto \frac{V^2}{\epsilon_d - \mu}. \tag{20}$$

10.7 The Luttinger Theorem and the Friedel Sum Rule

The Luttinger theorem states that the volume enclosed by the Fermi surface is conserved under electron interactions, depending only on the total electron count. At zero temperature, the Fermi surface remains well-defined, ensuring continuity between non-interacting and interacting systems.

Friedel Sum Rule The Friedel sum rule relates the scattering phase shifts of electrons near an impurity to the number of electrons bound by the impurity. For $l = 0$ (s-wave scattering), the phase shift η satisfies:

$$\Delta N = \frac{2\eta}{\pi}, \tag{21}$$

where ΔN is the number of bound electrons. This principle explains phenomena such as the unitary scattering in the Kondo effect and the formation of resonance peaks near the Fermi energy.

10.8 Conclusion

The models and concepts in this chapter provide the foundation for understanding interacting-electron systems. They highlight the interplay between kinetic and potential energies, the role of symmetry breaking, and the emergence of collective phenomena. These frameworks are essential for studying phenomena such as metal-insulator transitions, magnetism, and the behavior of strongly correlated materials.